

# Chapter 1

## Introduction

**Abstract** This chapter gives an introduction to interacting many-body systems. Interaction effects give rise to collective behavior, dominated by mean field effects, as well as to correlations. We start from classical systems in thermodynamic equilibrium and proceed to relaxation processes following an external excitation. Finally, we discuss ultrafast relaxation processes that have become of high interest in recent years in many fields of physics and quantum chemistry, due to the availability of very short light pulses. Our main conclusion here is that traditional many-body concepts based on kinetic equations of the Boltzmann-type fail badly: they lead (among other problems) to unphysically fast relaxations that are in conflict with experiments. This is illustrated on an example from semiconductor optics in Sect. 1.4. From this we come to the necessity to derive improved quantum-kinetic equations. This task is realized in the main part of this book along two lines: reduced density operators, Chaps. 2–12, and nonequilibrium Green functions, Chap. 13.

**Subject of this book.** This book is devoted to quantum systems of *many particles* in *nonequilibrium*. More precisely, we will be interested in *many-body effects* (collective and correlation effects) and, in particular, how these effects show up on *very short time scales*. What means “short” depends on the actual system, but also on the observer. For us, “short” and “ultrafast” will refer to the initial stage of relaxation, to *times shorter than the correlation time* of the system,  $t < \tau_{cor}$ , where the conventional statistical description, the traditional kinetic theory such as the Boltzmann equation, fails.

Why are these initial or transient processes of interest? The reason is the recent remarkable progress in short pulse lasers,<sup>1</sup> free electron lasers and other coherent radiation sources, which allow to excite and to probe many-particle systems during an extremely short time which is often comparable or even shorter than the correlation time. This yields deep insight into the behavior of matter under conditions very far from equilibrium which have not been accessible for systematic quantitative analysis before. For example, it is becoming possible to follow in detail the formation of a plasma, including the buildup of the screening cloud and of the correlations between the charge carriers.

---

<sup>1</sup>Laser pulses as short as 100 as =  $10^{-16}$  s are now available [1], see Sect. 1.3.2.

Theoretical studies of ultrafast processes started about two decades ago. Only recently systematic numerical investigations became possible, due to the progress in, both, theoretical approaches and computational resources. So this book discusses early and more recent results. More importantly, it outlines the some of the most important theoretical approaches to ultrafast relaxation phenomena: the density operator formalism, nonequilibrium Green functions and classical and quantum dynamics techniques. Our main focus will be on the first, which will be used to derive generalized quantum kinetic equations, which are applicable to correlated many-particle systems in general and to the initial stage of relaxation in particular.

Interestingly, related problems have been discussed already as early as in the 1950s by a number of authors in kinetic theory, plasma physics, fluid and condensed matter theory or nuclear matter. While these had to be purely theoretical studies, many contain brilliant concepts which are worth to be re-considered today, including possible extension beyond their original field of application.

## 1.1 Correlated Many-Particle Systems

**Many-body effects.** Before considering ultrafast relaxation phenomena in correlated systems, we briefly discuss the many-body (or nonideality) effects which govern their properties in equilibrium as well as in nonequilibrium. These are effects resulting from the mutual interaction<sup>2</sup> of the particles in the system. Their strength is naturally measured by the **nonideality parameter**  $\gamma_a$ —the ratio of mean potential to mean kinetic energy of particle species “ $a$ ”,

$$\gamma_a = \frac{|\langle V_a \rangle|}{\langle T_a \rangle}; \quad \langle T_a \rangle_{cl}^{EQ} = \frac{i_a}{2} k_B T; \quad \Gamma_a = \frac{e_a^2}{d k_B T} \quad (1.1)$$

where  $\langle T_a \rangle_{cl}^{EQ}$  denotes the classical mean kinetic energy in equilibrium,  $i_a$  is the number of degrees of freedom (which equals three for free elementary particles), and  $d$  denotes the mean interparticle distance which is defined via the density  $n$ , by  $4\pi d^3/3 = n^{-1}$ . For the important case of charged particles interacting via the Coulomb potential,<sup>3</sup>  $V_{ab}(r) = e_a e_b / \epsilon_b r$ , [ $\epsilon_b$  is the dielectric constant of the medium surrounding the charges  $e_a$  and  $e_b$ ], traditionally a slightly modified “coupling parameter” is being used which is denoted by  $\Gamma_a$  in (1.1). Throughout this book we will use  $\Gamma_a$ .<sup>4</sup>

The coupling parameter allows for a qualitative understanding of the behavior of nonideal many-body systems in equilibrium. For  $\Gamma \rightarrow 0$ , the system is ideal,

---

<sup>2</sup>Correlation effects exist also in non-interacting quantum systems where they arise from fermionic or bosonic exchange.

<sup>3</sup>Throughout this book, we use *Gaussian units*.

<sup>4</sup>Using (1.1), it is straightforward to extend the results for Coulomb interaction to systems with other pair interactions.

while for  $\Gamma < 1$  ( $> 1$ ) it is weakly (strongly) nonideal. This means, with increasing nonideality, all thermodynamic quantities will acquire interaction corrections, and the system behavior will increasingly deviate from that of an ideal gas. A microscopic picture of the role of interaction effects is obtained by considering the pair distribution function  $g(r)$ , i.e. the probability to find, for any given particle, a second particle at the distance  $r$ . This function is shown in Fig. 1.1, for a one-component Coulomb system in a broad range of  $\Gamma$ -values. In the absence of pair interactions the particles are independent of each other and, consequently,  $g(r)$  is distance-independent. For increasing (repulsive) interaction, the vicinity of each particle is empty—a so-called correlation hole forms which grows with  $\Gamma$ . At the same time, a pronounced peak emerges in the vicinity of the nearest neighbor distance.

**Phase diagram.** Interestingly, not only the short-range behavior of the pair distribution is influenced by interactions. For large  $\Gamma$  there emerges an obvious long-range structure in  $g(r)$  that is characteristic for liquid-like and crystal-like ordering. In fact, a first-order phase transition is well established in this system around  $\Gamma = 175$ , e.g. [15] which is directly linked to the height of the first peak of  $g(r)$  [16, 17]. We may now inquire for what densities and temperatures this behavior will be realized. To this end, we plot lines of constant  $\Gamma$ -values in the density-temperature plane, cf. Figs. 1.2

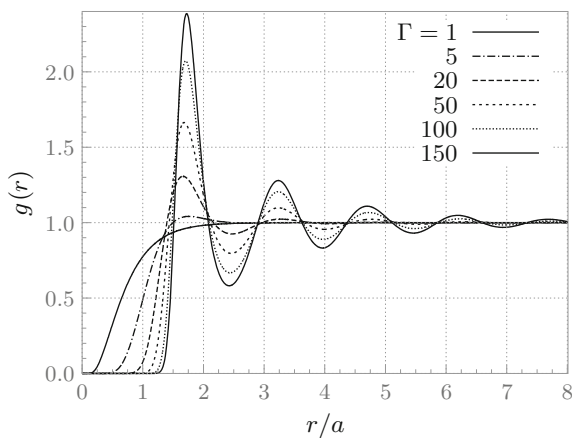


**Fig. 1.1** Pair distribution function of a one-component classical Coulomb plasma in thermodynamic equilibrium, for different values of the coupling parameter  $\Gamma$  that are indicated in the figure. The function  $g(r)$  is the probability to find an arbitrary particle pair at the distance  $r$  which is normalized to one,  $\int_0^\infty dr r^2 g(r) = 1$ . For an ideal system ( $\Gamma = 0$ ), this function would be a *straight line*,  $g(r) \equiv 1$ . Increasing correlations lead to formation (and expansion) of a “correlation hole” around zero particle separation as well as to the emergence of long-range liquid-like and crystal-like order, seen in oscillations of  $g(r)$  of increasing amplitude. The largest value of  $\Gamma$  is slightly below the crystallization transition. The pair distribution is computed by recording the distances  $r_{ij}$  of all particle pairs and averaging over all realizations:  $g(\mathbf{r}) = \frac{1}{Nn} \left\langle \sum_{i \neq j}^N \delta[\mathbf{r} - \mathbf{r}_{ij}] \right\rangle$  and, finally, averaging over all orientations. The results are obtained using first-principle molecular dynamics simulations. Distances are shown in units of the Wigner-Seitz radius. Figure courtesy of T. Ott

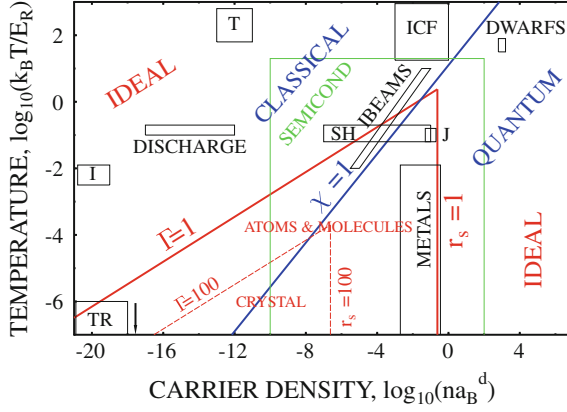


**Fig. 1.2** Strong coupling region of charged particles in equilibrium. The density-temperature plane is shown in system-independent dimensionless parameters ( $d$  is the dimensionality). The degeneracy parameter  $\chi$ , (1.2) divides the plane into classical and quantum systems whereas the classical and quantum coupling parameters,  $\Gamma$  and  $r_s$ , (1.1), (1.3) separate weakly coupled from strongly coupled systems. The short cuts of the example plasmas denote: SH: shocked plasmas, IBEAMS: ion beam compressed plasmas, T: tokamaks, ICF: inertial confinement fusion systems, J: plasma in the core of Jupiter, TR: nonneutral plasmas in traps, I: ion crystals, DWARFS: ion liquids and crystals in the core of *white* and *brown* dwarf stars. Reproduced with permission from [14]. Copyright (2003) by IOP Publishing. All rights reserved

and 1.4. The line  $\Gamma = 1$  gives a qualitative boundary to the region where nonideality effects are important, see Figs. 1.2 and 1.4. Obviously, many-particle systems are ideal at sufficiently high temperatures, but also at very low densities, because there the mean interparticle distance is large and  $\langle V_a \rangle \rightarrow 0$ . On the other hand, density increase results in an increase of the interaction energy and of the coupling parameter  $\Gamma$ . Obviously, this picture breaks down when two particles approach each other beyond the limit where quantum effects become important.

**Quantum effects. Degeneracy parameter  $\chi$ .** Quantum and spin effects will become important as soon as the mean interparticle distance  $d$  approaches the characteristic quantum extension of the particles which is characterized by the De Broglie wave length  $\lambda_{DB} = h/p$ , where  $p$  denotes the momentum. In thermodynamic equilibrium it is reasonable to use, for the momentum, the thermal momentum. Correspondingly, we define the quantum degeneracy parameter  $\chi$  as

$$\chi_a = n_a \Lambda_a^3 \sim \left( \frac{\Lambda_a}{d} \right)^3 \sim \left( \frac{E_{Fa}}{k_B T} \right)^{3/2} \equiv \Theta_a^{-3/2}; \quad \Lambda_a^2 = \frac{h^2}{2\pi m_a k_B T} \quad (1.2)$$

where  $\Lambda_a$  is called “thermal De Broglie wave length” of particle “a”. For  $\chi > 1$  (above the line  $\chi = 1$  in Figs. 1.2 and 1.4), the interparticle distance is smaller than  $\Lambda$ , i.e. particles “feel” their wave nature, and the system is essentially quantum or degenerate. Notice that these parameters are different for different particle species.

The degeneracy parameter sensitively depends on the particle mass: heavier particles become degenerate only at higher densities (lower temperatures) than light particles. From the definition (1.2) it is obvious that the degeneracy parameters of two particle species scale with their masses as  $\chi_a/\chi_b = (m_b/m_a)^{3/2}$ . For the example of hydrogen this means that proton degeneracy parameter is approximately 80,000 times smaller than the one of the electrons. In (1.2) we also indicated that the degeneracy parameter can be expressed in terms of  $\Theta$ —the ratio of two characteristic energies: the thermal energy and the Fermi energy (defined below). This latter expression applies only to fermions (see Problem 1.1, Sect. 1.6).

Note that the choice of the thermal De Broglie wavelength applies only to free fermions and bosons. In the case of bound particles (e.g. electrons in atoms) the proper length scale is the extension of the bound state wave function. Similarly, for quantum particles confined by some trapping potential the extension of the wave function is determined by the confinement. In the case of a harmonic oscillator, the proper scale is the oscillator length  $l_0^2 = \hbar/(m\omega)$ .

**Correlation effects in quantum systems.** To estimate correlation effects in the case of quantum degeneracy we have to redefine the coupling parameter, (1.1). Most importantly, the mean kinetic energy has to be evaluated using the correct Bose or Fermi statistics. In the case of fermions one obtains [ $\beta \equiv 1/(k_B T)$ ]

$$\langle T_a \rangle_q^{EQ} = \frac{i_a}{2} k_B T \frac{I_{3/2}(\beta \mu_a^{id})}{I_{1/2}(\beta \mu_a^{id})}; \quad \Gamma_{qa} \equiv \left( \frac{\hbar \omega_{pa}}{E_{Fa}} \right)^2 \sim r_s \equiv \frac{d_a}{a_B} \sim n_a^{-1/3} \quad (1.3)$$

where  $\langle T_a \rangle_q^{EQ}$  denotes the mean quantum kinetic energy in equilibrium, involving the Fermi integral,  $I_\nu$  [see Appendix A], and  $\mu_a^{id}$  the ideal chemical potential.<sup>5</sup> In (1.3) we also defined two commonly used coupling parameters that refer to a Fermi system at zero temperature: the quantum coupling parameter  $\Gamma_q$  that involves the plasma frequency,  $\omega_{pa}^2 = 4\pi n_a e_a^2/m_a$ , and the Fermi energy,  $E_{Fa} = \frac{\hbar^2}{2m_a} (3\pi^2 n_a)^{2/3}$ . One readily verifies the direct proportionality  $\Gamma_q \sim r_s$ , where  $r_s$  is the so-called **Brueckner parameter**, and  $a_B$  is the Bohr radius,<sup>6</sup>  $a_B = \frac{\hbar^2}{e^2 m_e}$  (see Problem 1.2, Sect. 1.6).

It is interesting to note that the quantum Coulomb coupling parameter (we will use  $r_s$ , in the following) scales with density according to  $r_s \sim n^{-1/3}$ . This means, a Coulomb interacting quantum system becomes ideal, with increasing density. This trend, which is in contrast to the classical behavior, arises from the strong density dependence of the quantum kinetic energy (which equals 3/5 of the Fermi energy)

<sup>5</sup>The ideal chemical potential is given by  $\chi_a = I_{1/2}(\beta \mu_a^{id})$ , where  $\chi_a$  is the degeneracy parameter (1.2).

<sup>6</sup>The Bohr radius is straightforwardly generalized to hydrogen-like bound states of two arbitrary particles with charges  $e_a$  and  $e_b$  and masses  $m_a$  and  $m_b$ , according to  $a_B^H = \frac{\epsilon_b \hbar^2}{e_a e_b m_{ab}}$ , where we introduced the reduced mass,  $m_{ab} = m_a m_b / (m_a + m_b)$ , and the background dielectric constant,  $\epsilon_b$ , is included to allow for a medium surrounding the bound states.

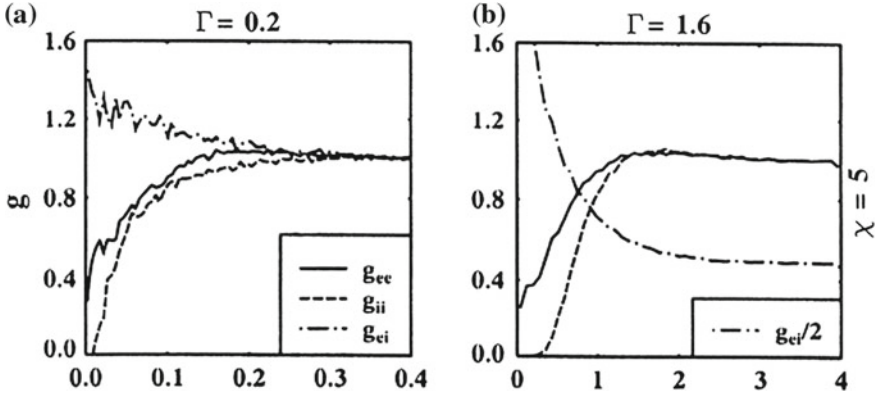


**Fig. 1.3** Pair distribution function of a dense two-component electron-ion plasma (hydrogen) in thermodynamic equilibrium in the quantum regime (for the electrons,  $\chi = 5$ ). The three curves correspond to the three types of particle pairs. The Coulomb repulsion between two electrons and two ions gives rise to the “Coulomb hole” at small distances, exactly like in the one-component case, cf. Fig. 1.1. Note that this hole is narrower for electrons which is due to quantum degeneracy (finite extension of the electron wave functions). The Coulomb attraction between electrons and ions gives rise to a maximum of  $g_{ei}$  around  $r_{ie} = 0$ . The two plots correspond to two values of the Coulomb coupling parameter  $\Gamma$ , at constant electron degeneracy parameter  $\chi = 5$ . The corresponding densities and temperatures are: **a**  $T = 60.5 E_R$ ,  $n = 3.57 \cdot 10^{26} \text{ cm}^{-3}$  [ $r_s = 0.17$ ] and **b**  $T = 0.94 E_R$ ,  $n = 7 \cdot 10^{23} \text{ cm}^{-3}$  [ $r_s = 1.4$ ]. The results are obtained using path integral Monte Carlo simulations. Distances are given in units of the Bohr radius  $a_B$ , the temperature scale is one rydberg,  $1 E_R = 13.6 \text{ eV}$ . Figure reprinted from [18], Copyright (2000), with permission from Elsevier

that grows faster than the mean interaction energy (which grows only as  $n^{1/3}$ ).<sup>7</sup> It is instructive to look at the pair distribution function (PDF) of a nonideal system in the quantum regime. Figure 1.3 shows the three pair distributions of a dense hydrogen plasma  $g_{ee}(r)$ ,  $g_{ii}(r)$  and  $g_{ei}(r)$ , for weak [(a):  $r_s = 0.17$ ] and moderate [(b):  $r_s = 1.4$ ] coupling, respectively. As in the classical case, with increasing coupling, the Coulomb hole increases, cf. the ion-ion PDF. Note that the Coulomb hole is smaller for the electrons, compared to the ions. This is due to the larger spatial extension of the electrons which reduces the  $e-e$  repulsion whereas the ions are still almost point-like. At weak coupling [cf. Fig. 1.3a], the electron-electron PDF is strongly affected by fermionic exchange. In the limit of an ideal Fermi gas, due to the Pauli principle, two electrons with the same spin projection cannot occupy the same position, i.e.  $g_{ee}^{\uparrow\uparrow}(0) = 0$ , whereas two electrons with opposite spin will be nearly independent,  $g_{ee}^{\uparrow\downarrow}(0) = 1$ . Therefore, the total PDF which is the superposition of these cases approaches, for  $r_s \rightarrow 0$ , the value  $g(0) = 0.5$ , which is in good agreement with the numerical result in Fig. 1.3a.

**Coulomb bound states.** In two-component charged particle systems, another nonideality effect is the formation of bound states—atoms, molecules, clusters etc.

<sup>7</sup>Strictly speaking, this is true only for fermions and in the non-relativistic limit.

Solving the quantum-mechanical bound state problem [we consider hydrogen, as an example<sup>8</sup>] yields the characteristic binding energy spectrum, with the ground state energy  $E_{1s} = -E_R = -13.6\text{ eV}$  corresponding to a mean electron-proton distance equal to  $a_B$ . The average extension of a bound electron is of the same order, i.e.  $\Lambda_e^{\text{bound}} \simeq a_B$ .

Now the interesting question is how bound states will be modified if they are embedded into a many-particle system in thermodynamic equilibrium. In other words: for what temperatures and densities will bound states exist? The first effect is that of temperature. With increasing temperature, electrons bound in atoms will acquire additional kinetic energy, and already for  $k_B T \gtrsim 0.2E_R$  the probability to leave the binding potential will be finite. Correspondingly, the degree of ionization (fraction of free electrons) will be significant (thermal ionization). An analogous mechanism exists in a quantum plasma if the system is being compressed. If the mean interparticle distance becomes comparable to the Bohr radius, i.e.  $r_s \sim 1$ , electron wave functions from neighboring atoms will start to overlap, and electrons can tunnel out of the atom. This process which occurs even at zero temperature is called pressure ionization (or Mott effect). This qualitative picture has been confirmed by first principle path integral Monte Carlo simulations [19, 20], where the critical density (Mott density) for the break up of atoms<sup>9</sup> was found to be  $r_s \approx 1.2$ .

**“Corner of correlations”.** The dependence of the coupling strength on density and temperature is summarized in Fig. 1.2. One clearly sees that nonideality effects are enclosed between the two lines  $\Gamma = 1$  and  $r_s = 1$ . This means that correlation effects, liquid and solid behavior that was discussed above, are confined to this triangular area. For example, crystal-like long-range ordering in quantum systems is observed for  $r_s \gtrsim 100$ , e.g. [15]. It is this “*corner of correlations*”<sup>10</sup> where the structure of matter differs from the trivial state of nearly independent elementary particles or of the ideal quantum Bose or Fermi gas. This region contains all cooperative phenomena—from simple bound states such as atoms, excitons or nuclei, to living organisms.

While we have considered so far a hydrogen plasma, as an example, the correlation effects discussed above are essentially universal in charged particle systems. Details of the specific system, such as the charges and masses of the constituents and properties of the background medium (e.g. the background dielectric function  $\epsilon_b$ ) are “absorbed” in the dimensionless coupling parameters,  $\Gamma_a$ ,  $r_{sa}$  and the degeneracy parameter  $\chi_a$ . Thus, the phase diagram and the characteristic phase boundaries shown in Fig. 1.2 have an almost universal form.

Naturally, for two specific system, the phase boundaries will be displaced from each other if one uses, instead, dimensional densities and temperatures which is done in Fig. 1.4. The range of temperatures and densities where charged particles exist is astonishingly broad. Aside from plasmas occurring in the universe or in laboratory

<sup>8</sup>It is straightforward to extend this to other hydrogen-type bound states by properly rescaling the Rydberg energy  $E_R$  and the Bohr radius.

<sup>9</sup>This was defined by the density where the degree of ionization reaches 10 %.

<sup>10</sup>The term was introduced by Ebeling et al. [21].

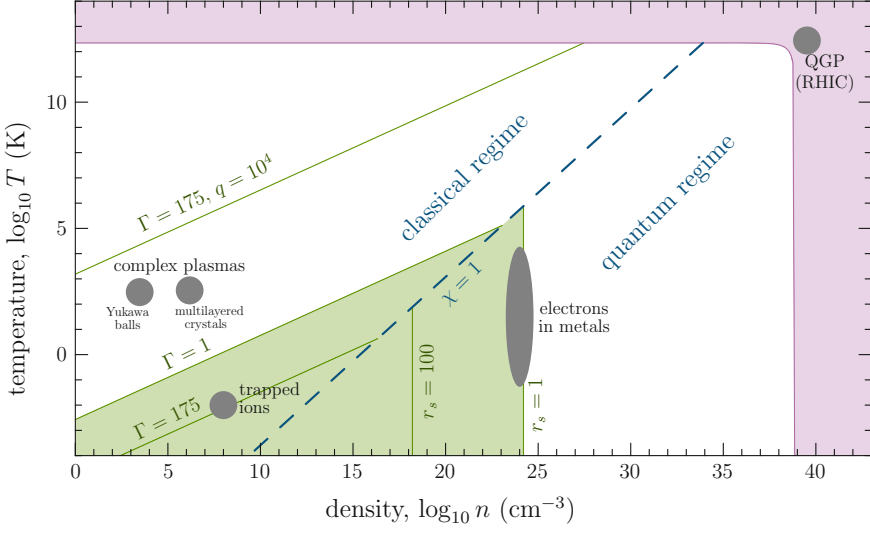


**Fig. 1.4** Extended density-temperature plane of a one-component charged particle system. The dimensionless form of Fig. 1.2 is here converted into dimensional densities and temperatures. The “corner of correlations” (bounded by the lines  $\Gamma = 1$  and  $r_s = 1$ ) is shown by the green area. The pink layer marks the region of break up of nuclear matter either at high temperature exceeding the deconfinement temperature or at high density (see text). QGP denotes the quark gluon plasma that has been produced in heavy ion collisions at Brookhaven National Laboratory and at CERN. From [22]

setups there exists a variety of artificial “non-neutral” plasmas which are confined by external potentials. Examples are electrons in semiconductor quantum dots, ions in traps or complex (dusty) plasmas. In the latter case, the charged particles carry between thousand and one hundred thousand elementary charges giving rise to huge coupling parameters. As a result the phase boundaries (lines of constant  $\Gamma$ ) move up to high temperatures.

**Ultra-high temperature or densities.** If the temperature is increased beyond the atomic binding energy, electrons are freed one by one from molecules and atoms, and the system transforms into the fully ionized plasma state. For the case of atoms with charge number  $Z$ , this process continues until all  $Z$  electrons are ionized and a  $Z$ -fold charged nucleus is left. An analogous sequence of transitions is observed for a density increase, along lines of constant temperature. If  $r_s$  becomes smaller than 1.2, atoms break up via tunnel ionization. Further compression will lead to the break up of ions until only electrons and bare  $Z$ -fold charged nuclei remain.

Further temperature increase (or compression) will ultimately lead to kinetic energies that are sufficient for protons and neutrons to leave the atomic nucleus. This occurs at densities for which the average distance between two nuclei becomes of the order of the average distance of nucleons in the atomic nucleus. The average density of nuclear matter is about  $n_{\text{NM}} = 0.16 \text{ fm}^{-3} = 0.16 \cdot 10^{39} \text{ cm}^{-3}$ , where



one Fermi (or femtometer) equals  $1 \text{ fm} = 10^{-13} \text{ cm}$ . Even this is not the end of the story: At further compression, nucleons will break up into quark triplets. The same processes of deconfinement of quarks occurs at ultrahigh temperatures, where the deconfinement temperature has been established to be around  $T_d \simeq 175 \text{ MeV}$ . The quark deconfinement transition is depicted by the pink band in Fig. 1.4.

## 1.2 Thermodynamic Properties of Correlated Systems

Although equilibrium properties are not our main subject, it is important to understand the effect of correlations first for this simplest case. The simple reason is that the thermodynamic equilibrium state is often the end point of relaxation processes of a system that is externally excited. In this case a key requirement for the theory of the nonequilibrium dynamics should be that it guarantees that the evolution converges to the correct thermodynamic state.

In a correlated system, the ground state as well as the thermodynamic equilibrium state may be strongly modified compared to an ideal gas. In particular, the thermodynamic functions, such as free energy, internal energy, chemical potential, pressure and so on contain additional interaction contributions, e.g.  $F = F^{\text{id}} + F^{\text{nonid}}$ ,  $\mu = \mu^{\text{id}} + \mu^{\text{nonid}}$ .

**Energy of the electron gas.** As an example, we consider the total energy of the uniform electron gas (“jellium”). This model system has been well studied theoretically, and there exist many semi-analytical fits for the energy as a function of  $r_s$ , see [23], for an overview. In addition, benchmark results have been produced using path integral Monte Carlo (PIMC) simulations, e.g. [24]. These data have been of central importance for applications to real materials because the total energy for  $T = 0$  serves as a key input for density functional theory simulations. Here we extend this to finite temperatures which is currently of substantial importance to highly excited materials, as well as to dense plasmas (“warm dense matter”). In Fig. 1.5 we show PIMC results for the total energy of the uniform electron gas at a finite temperature corresponding to  $\Theta = 0.0625$ . The left part shows the total energy as the function of the Brueckner parameter  $r_s$ , compared to the energy of an ideal Fermi gas. The difference between the two—the correlation energy—is plotted in the right figure. It is obvious that correlation contributions play a crucial role for this system. The discrepancy between the two sets of simulations indicates that these quantities are still under investigation, in particular in the range of low  $r_s$ . Additional simulations that are more accurate for weakly coupled electrons ( $r_s < 1$ ) have been reported by Schoof et al. [25, 26] using the recently developed configuration PIMC approach [27].

**Partial ionization. Chemical composition.** Correlation effects may have a drastic impact on the equation of state  $p = p(n, T) = p^{\text{id}} + p^{\text{nonid}}$ , as well as on the chemical composition of partially ionized or partially dissociated systems. Figure 1.6 shows, as an example, the chemical potential of electrons and protons in a partially ionized hydrogen plasma. At low densities the plasma is fully ionized and electrons and

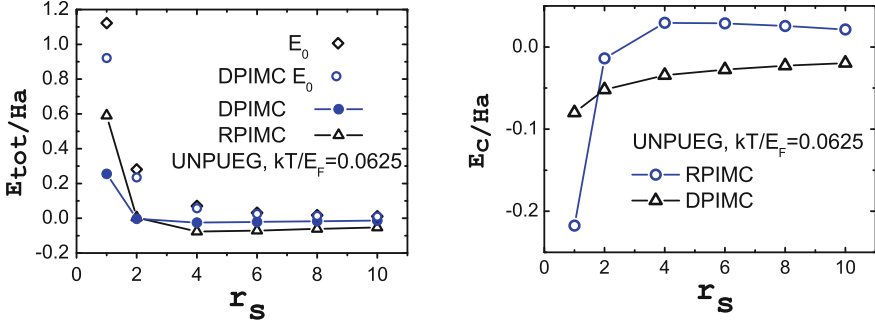


**Fig. 1.5** Energy of the uniform unpolarized degenerate electron gas (jellium) at a finite temperature,  $\Theta = k_B T/E_F = 0.0625$ .  $E_0$ : ideal energy. DPIMC: direct fermionic PIMC simulation; RPIMC: restricted PIMC [28]. All energies are in units of Hartree ( $1H_a = 2E_R$ ). **Left figure**: Total energy; **Right figure**: Correlation energy. Reprinted with permission from [29]. Copyright (2015) by the American Physical Society

protons behave classically ( $\chi_e < 1$ ), as can be seen in Fig. 1.4. The chemical potential shows the behavior well-known for an ideal gas,  $\beta\mu \sim -\ln n\Lambda^3$ . In contrast, at high densities,  $n \gtrsim 10^{24} \text{ cm}^{-3}$ , we observe the behavior resembling an ideal Fermi gas where  $\beta\mu \sim I_{-1/2}(\chi)$ . For the density region between these two limits correlation effects are important, at low temperatures. Indeed, this density interval is just inside the “corner of correlations”, see above. Correspondingly, we observe a lowering of the chemical potential below the ideal curve,<sup>11</sup> as in the case of the energy of the electron gas above, cf. Fig. 1.5.

In the present case of a plasma with attractive interactions the strongest correlation effect is the formation of atoms and molecules. This can be described theoretically using a chemistry-motivated approach: formation of an atom is described as a chemical reaction of the recombination of an electron and a proton.<sup>12</sup> In thermodynamic equilibrium the chemical composition follows from the condition of equal chemical potentials of the reactants. For example, the detailed balance in the ionization/recombination of atomic hydrogen as well as molecular dissociation is given by  $\mu_e + \mu_p = \mu_H$ , and  $2\mu_H = \mu_{H_2}$  where all chemical potentials contain interaction contributions. This leads to the mass action law (Saha equation) for nonideal systems which is readily solved numerically for the density of free electrons (degree of ionization) [32]. Results for hydrogen are shown in Fig. 1.6 along various isotherms. At low densities, first atoms are formed, whereas molecules appear at higher densities. All bound states vanish due to weakening of the binding energy in the plasma (screening and quantum effects) leading to pressure ionization (Mott effect), as was

<sup>11</sup>The intermittent monotonic decrease of the chemical potential as a function of carrier density may be related to a phase transition (the hypothetical plasma phase transition) [30], for a discussion, see e.g. [31, 32]. This issue is still controversially discussed, e.g. [33, 34] including recent predictions of a substantially lower critical temperature [35].

<sup>12</sup>This is just the net balance. The true process is, of course, three-body recombination or photo-recombination.

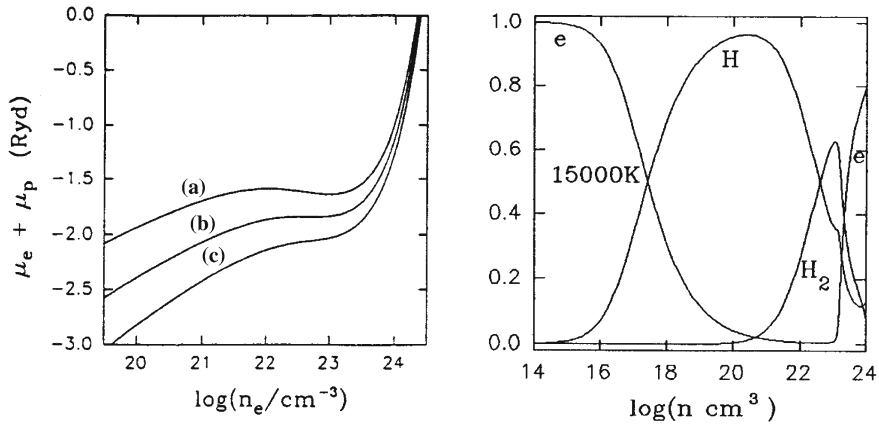


**Fig. 1.6** Chemical composition of partially ionized hydrogen. **Left figure:** Correlated equilibrium chemical potentials of electrons and protons (divided by  $k_B T$ ) versus free electron density, for  $T = 14,000\text{ K}$  (a),  $17,000\text{ K}$  (b) and  $20,000\text{ K}$  (c). The minimum is due to correlations, ( $1\text{ Ryd} = E_H = 13.6\text{ eV}$ ). **Right figure:** Fractions of electrons which are free or bound in atoms or molecules versus total electron density. The region of bound states indicates the influence of correlations. At high densities the *effective binding energy*  $I^{\text{eff}}$  of atoms and molecules decreases due to screening, and bound states are no longer stable (Mott effect, see text). Reprinted with permission from [32]. Copyright (1995) by WILEY

discussed above. Similar effects are found in partially ionized electron-hole-exciton plasmas in semiconductors, e.g. [21, 36], and in nuclear matter.

The main task to compute the chemical composition consists in finding appropriate approximations for the interaction contributions of the chemical potentials of electrons, protons, atoms and molecules. While this is rather successful at low and high density, fundamental difficulties in this “chemical picture” [8, 21, 31] arise in the intermediate density range that is shown in Fig. 1.6. Here the distinction between bound and free particles is, to some degree, arbitrary, and a more appropriate approach is the “physical” picture where no such subdivision is introduced. Examples are thermodynamic (Matsubara) Green functions methods, e.g. [8] and quantum Monte Carlo, e.g. [37, 38]. In the former, bound and free electrons are described by a single Green function (spectral function), and appear in different parts of the spectrum. In the latter, only elementary particles (electrons and protons or electrons and holes in semiconductors) are simulated, and bound states appear “spontaneously” as spatially tightly bound pairs of elementary particles, see below.

**Theoretical approaches to equilibrium properties.** Following these examples, we now list important theoretical methods that were developed in recent years to describe the equilibrium properties of correlated many-particle systems.<sup>13</sup> We first list methods for classical systems.

<sup>13</sup>This list is by no means complete but rather based on personal experience of the author.

1. *Integral equation techniques*: These techniques and approximations such as the hypernetted chain (HNC) approximation have been developed in the theory of classical fluids and have proven to be very efficient to describe strong correlation effects, also in partially ionized dense plasmas. For a text book overview see [39];
2. *Stochastic modeling*: First principle simulations of classical nonideal equilibrium systems are possible using Monte Carlo methods, following the classical algorithm of Metropolis et al. [40] or similar concepts, for an overview see [38, 41];
3. *Dynamic (classical or quantum mechanical) modeling*: Molecular Dynamics techniques allow to perform first-principle simulations for classical systems by solving Newton's equations with a suitable thermostat. Thermodynamic quantities are computed using Green-Kubo-type (fluctuation dissipation) relations. For details see, e.g. [42].
4. *Variational quantum approaches*: Various methods, in particular, Thomas-Fermi theory and density functional theory [43] are very successful in many fields of physics and chemistry, including condensed matter, materials and complex systems. The difficulty here is the treatment of finite temperatures and of correlation effects.
5. *Quantum statistics*: Field-theoretical concepts such as equilibrium (Matsubara) Green functions theory involving diagrammatic expansions are particularly successful, for textbook discussions of these methods, see [8, 21, 31, 44, 45]. An introduction is presented in Chap. 13;
6. *Density operators*: This is the main topic of this book, and the special case of equilibrium density operators and correlation functions is briefly covered in Sect. 2.7;
7. *Path integral methods*: Here the idea is to evaluate the  $N$ -particle density operator. For an overview, see the classical monographs of Feynman and Hibbs [46] and Kleinert [47]. Modern applications of this interesting approach to quantum systems concentrate on path integral Monte Carlo methods. Some results were presented in Figs. 1.3 and 1.5 above, for an overview see [38].

These methods are often highly specialized for the investigation of equilibrium properties of various many-particle systems. For more details and further references, see e.g. [31]. But we will see below that not all of these concepts are applicable to situations far from equilibrium.

### 1.3 Ultrafast Nonequilibrium Phenomena

Let us now assume that our equilibrium  $N$ -particle system at some moment  $t = t_0$  is influenced by an *external excitation*. This can be the compression of the system, a heating process, the penetration of a particle beam into the system or the applications of an external field. As a result, the system will respond to the excitation—by reaching a new pressure, temperature or chemical composition, or it will adapt by assuming a new charge distribution—until it, eventually, comes to a new equilibrium state. It is the main subject of *nonequilibrium theories*, to understand this relaxation process

and to predict how the final state will look like. Based on this knowledge, one may suggest a specific form of excitation which allows to reach a well-defined desired state.

Thus, nonequilibrium theories have to solve two problems: (1) What are the properties of various external excitations, what are their time scales, how do they interact with the particle system and how much energy in what spectral composition do they allow to “feed” into the system? And (2), what are the dominant *relaxation mechanisms* in a given many-particle system, how can they be activated, how much momentum and energy do they allow to transform? Obviously, both questions are closely related and require a detailed knowledge of the microscopic properties of many-particle systems and of the character of the interaction of the particles with the excitation under nonequilibrium conditions.

Before answering these questions we briefly consider a different case—that of an isolated system. This has, traditionally been considered an idealized case, because effects of the coupling to the environment are always thought to be present. However, in recent years isolated few-particle systems have come into the focus of various experiments and stimulated theoretical developments. We return to the issue of relaxation processes in Sect. 1.3.2.

### 1.3.1 Dynamics of Isolated Systems

Electrons in an atom can be easily excited by an electromagnetic field. In many cases their dynamics is very weakly coupled to the environment. This means these dynamics are (almost) dissipationless and time-reversible and can be studied theoretically using standard quantum mechanics in the framework of the Schrödinger equation. For the coupled dynamics of several electrons this equation is numerically very challenging, and exact solutions (exact diagonalization or “configuration interaction”, CI) are limited to simple problems. In addition, in physics and quantum chemistry, numerous approximate solution schemes have been developed that allow for time-dependent solutions for the dynamics of correlated electrons. A recent overview on various methods can be found in [48].

Another type of isolated few-body system are ultracold atoms in optical lattices. There has been remarkable experimental and theoretical progress in this field over the last decade which, however, is outside the focus of the present book. Here we note that the methods being in the focus of the present book—density operators and nonequilibrium Green functions—are well suited to study these systems as well. Among recent references discussing such applications we point out [11] and [49] and references therein.

Isolated pure state dynamics is, of course, a model situation. Already in the case of small molecules and, much more importantly, in larger aggregates of atoms such as clusters or condensed matter systems, the electron dynamics are not isolated but coupled to other degrees of freedom such as inter-nuclear vibrations, phonons and

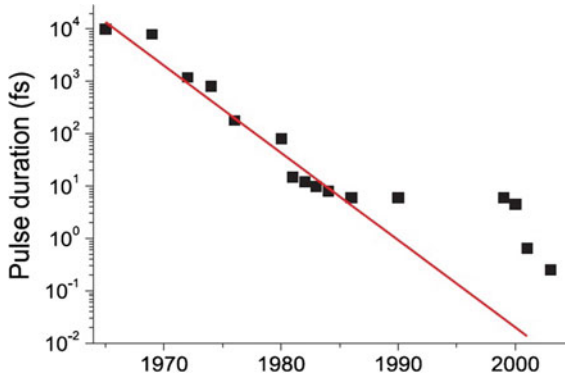


**Fig. 1.7** Duration of the shortest available laser pulses of the recent half century. The recent 15 years have witnessed a dramatic decrease of pulse durations to about 100 as, which is achieved by high-harmonics generation. This time is comparable with characteristic electronic scales in atoms and condensed matter. Such pulses will allow to study electronic processes in atoms, molecules and materials. Reprinted with permission from [1]. Copyright (2008) by the Canadian Science Publishing or its licensors

other quasiparticles. This will, ultimately, lead to a loss of quantum coherence, to dissipation or dephasing. This is the situation we will be studying below.

### 1.3.2 Interaction of Matter with Short Laser Pulses

**Femtosecond and attosecond lasers.** To be more specific, we will mainly be interested in the excitation of correlated matter by *electromagnetic fields*, including longitudinal electric fields and the radiation field of a laser or free-electron laser (FEL). Especially lasers have, due to recent developments become a quite unique excitation source, supplying energy in an extraordinarily wide range of time duration, photon energy and power (intensity). Of particular importance is the availability of ultra-short radiation pulses. The development of pulse durations of the recent half century is illustrated in Fig. 1.7. While the first lasers had pulse durations in the range of nanoseconds to picoseconds, pulse durations fell continuously to about 6 fs, in 1986 [2] after which they remained nearly constant over 15 years.

The next breakthrough came in the early 2000s with the use of high-harmonics generation that brought pulses down to about 100 as, e.g. [1]. These are fields with photon energies in the ultraviolet (several tens of eV) of rather low intensity. An alternative route to short pulses in the UV to soft x-ray range is provided by FEL

radiation.<sup>14</sup> While these fields have higher intensity, the pulse durations are still in the range of a few to several ten femtoseconds.

Low-intensity lasers, mostly in the visible and infrared range, have been a key tool for time-resolved studies of semiconductors for a long time, e.g. [50, 51], where picosecond and femtosecond pulses have provided detailed information on the microscopic properties of bulk materials and low-dimensional nanostructures. XUV pulses are used to diagnose dense plasmas using Thomson scattering [52]. The reason is that these pulses have a duration which is comparable to typical response and relaxation times in these materials. With the availability of femtosecond and attosecond pulses completely new regimes are becoming accessible. It is now becoming possible to probe the electron dynamics in atoms where characteristic time scales are on the order of 20 as. With pulses of a few femtoseconds duration one can study the dynamics of chemical reactions involving molecules. Similar time scales are of relevance for electronic processes in condensed matter. Thus, accurate time resolved measurements are now a key tool for both fundamental research and technological applications. At the same time short-pulse lasers allow not only to probe but also to excite matter into a strong nonequilibrium state in a very well defined way.<sup>15</sup>

Finally, we mention a different route of progress—the evolution towards higher field intensities. Starting in the 1980s novel technical concepts,<sup>16</sup> have allowed to steadily increase the power concentrated in a single pulse to terawatts and petawatts ( $10^{12} \dots 10^{15}$ ) W and the corresponding intensities to the range of  $10^{19} \dots 10^{22}$  W · cm<sup>-2</sup>. The associated electromagnetic field strength by far exceeds the binding energies of solids and even that of heavy atoms. As a result it is possible to ionize any atom, up to Uranium, within the duration of a single oscillation cycle. This has an exceptional potential for many applications, including generation of relativistic electron and ion beams, the study of nuclear reactions, creation of electron-positron pairs, creation of ultradense matter or inertial confinement laser fusion.

Figure 1.8 summarizes the range of temporal and energetic parameters of laser pulses and compares them to relevant scales of various materials. Typical binding energies of different systems are shown in the right part of the figure.

**Field–matter interaction processes.** This interaction is readily understood within the photon picture: Field energy can be absorbed by matter in portions of  $\hbar\omega$ . The photon energy determines what kind of absorption process is possible, while the field intensity determines the average number of photons which can interact with the material simultaneously. Obviously, multiphoton processes become relevant only at sufficiently high intensities. On the other hand, there is the inverse mechanism possi-

<sup>14</sup>This remarkable development was achieved using the SASE (Selfamplification by spontaneous emission) scheme where coherent radiation with photon energies from the UV to soft X-rays has become available.

<sup>15</sup>The photon energy, laser intensity and pulse duration can be chosen accurately in a broad parameter range.

<sup>16</sup>This includes, in particular, “chirped” pulse amplification, where the frequency of the field varies in time. One succeeds in generating very short and intense pulses without damage to the optical system by dispersively stretching the pulse, and compressing it again only after amplification [53].

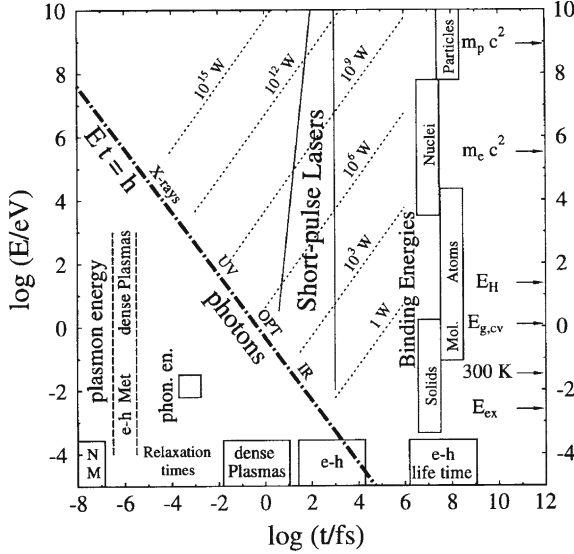


**Fig. 1.8** Typical energy and time scales of relaxation in various systems. *Along right border* range of binding energies of solids, atoms, molecules, nuclei and elementary particles, arrows correspond to excitons (ex), hydrogen (H), electron and proton rest mass and typical band gap in semiconductors. *Along left border* typical energies of photons and plasmons in semiconductors (e-h), metals and dense plasmas. *Along lower border* life time of e-h plasmas and typical relaxation time in semiconductors, dense plasmas and nuclear matter (for different densities, increasing inside each box from right to left). *Dash-dotted line* corresponds to Heisenberg's principle: for a given observation time, the energy uncertainty is above (or on) this line. At the same time, this line relates energies and oscillation periods for photons (frequency ranges are indicated). *Dotted lines* indicate constant power (in Watts). The *laser* area indicates energy versus pulse duration (below one picosecond) of modern lasers

ble, where particles emit radiation. There is a large variety of interaction mechanisms, among them are

- (i) *free charge acceleration* in the oscillating electric field of the wave: The average oscillation energy of an electron ("quiver" or ponderomotive energy) in the field of amplitude  $E$  and frequency  $\omega$  follows from Newton's equation<sup>17</sup>:  $U_{\text{pond}} = e^2 E^2 / (4m_e \omega)$ . With modern high-intensity lasers electrons are easily accelerated up to relativistic energies<sup>18</sup>;
- (ii) *carrier-photon scattering*: In scattering processes with photons electrons may gain (lose) energy, re-emitting a photon of lower (higher) energy (Thomson scattering). At relativistic energies this process is called "Compton scattering", which may also involve multiple photons;

<sup>17</sup>See Problem 1.3, cf. Sect. 1.6.

<sup>18</sup>For a laser wavelength  $\lambda = 1 \mu\text{m}$  and an intensity of  $10^{13} \text{ W/cm}^2$ ,  $U_{\text{pond}} \approx 1 \text{ eV}$ , the electron rest mass (about  $0.5 \text{ MeV}$ ) is reached at an intensity of  $1.37 \cdot 10^{18} \text{ W/cm}^2$ , see e.g. [54]. The relativistic average oscillation energy is  $E_{\text{osc}} = m_e c^2 ([1 + U_{\text{pond}}/m_e c^2]^{1/2} - 1)$  [55].



- (iii) *excitation of collective plasma oscillations* of the charge carriers: This is an efficient absorption mechanism for photons with an energy in resonance with the plasma (Langmuir) frequency  $\omega_{pl}^2 = (4\pi ne^2/m)$  or, similarly, for other collective plasmon modes. At high laser intensities the plasma wave will have very high field amplitudes and may itself act as an accelerator for electrons (“wake field” accelerator);
- (iv) *emission of radiation by moving charges*: Freely moving charges emit Cherenkov radiation<sup>19</sup> while charges which are slowed down, e.g. in the field of an ion, emit “bremsstrahlung”<sup>20</sup>;
- (v) *excitation processes* in atoms or molecules or *interband transitions* in solids: This is the most important mechanism at low field intensities, which is widely used in spectroscopy of atomic or condensed matter systems. The excited electrons gain a kinetic energy of  $E_{kin} = \hbar\omega - \Delta E$ , where  $\Delta E$  is the energy difference of the final and initial energy level;
- (vi) the inverse processes of (v): *de-excitation* of bound particles or interband transitions to lower lying bands which is associated with the emission of a photon. These processes may occur spontaneously or coherently by many electrons, where it leads to lasing;
- (vii) *Ionization of atoms or molecules*: If in (v) electrons are excited into the continuum, bound states become ionized. The kinetic energy of electrons and ions is given by  $E_{kin} = \hbar\omega - I^{\text{eff}}$ , where the ionization potential  $I$  may be modified by medium effects (screening, selfenergy etc. [56]);
- (viii) Ionization of condensed matter: Similarly as in the case of atoms, photons may kick out one or several electrons from a solid. The photoelectrons can be accurately detected, and their energy spectrum gives detailed information on the band structure of the material<sup>21</sup>
- (ix) *Multi-photon ionization*: At high intensities, multiple photons may be absorbed simultaneously by the atom to bridge the ionization gap. On the other hand, ionization is possible also off-resonance [57]: for photon energies below the gap (“tunnel ionization”) and also far above the gap (“above threshold ionization”). The kinetic energy of the electrons is  $E_{kin} = n\hbar\omega - I^{\text{eff}} - U_{\text{pond}}$ ;
- (x) *Relativistic photon–particle transitions*: Photons with energies above  $2m_e c^2 \approx 1 \text{ MeV}$  ( $\gamma$  quants) may generate electron-positron pairs. On the other hand, one also expects pair creation from lasers of ultra-high intensity in multi-photon processes,<sup>22</sup> e.g. [54].

Obviously, at relativistic energies a clear separation of some processes is no longer possible. There, a unified treatment of charge carriers and electromagnetic radiation is necessary, which is given by relativistic quantum electrodynamics (see Chap. 13).

---

<sup>19</sup>Charges moving with the velocity  $v$  emit radiation of frequency  $\omega$  and wave vector  $k$  on a cone around  $\mathbf{v}$ ,  $\omega = \mathbf{v} \cdot \mathbf{k}$ .

<sup>20</sup>For sufficiently high velocities, the frequencies easily reach the range of x-rays.

<sup>21</sup>The method of angle-resolved photoelectron spectroscopy (ARPES) is a powerful tool for basic physics and material science.

<sup>22</sup>Pair creation in a two-photon process was already discussed by Breit and Wheeler [58].

**Modifications on short times.** As noted before, traditional concepts have to be revised if ultrafast processes are being considered. The most striking effect results from *Heisenberg's uncertainty principle*: The picture of electromagnetic radiation consisting of portions with a sharp energy  $\hbar\omega$  breaks down on short times. Laser pulses with a duration of only a few femtoseconds or a hundred attoseconds which, in the optical range, corresponds to only a few oscillation periods, consist of photons which are “smeared out” energetically. [The corresponding relation between energy and time scales is shown in Fig. 1.8 by the line  $Et = h$ : For processes with a given time duration  $t$ , the minimal energy uncertainty is given by the crossing point with this line, and real processes are confined to the range above this line.] Instead of a photon with a fixed energy, an electron or atom will interact with radiation in a broad spectral range around  $\hbar\omega$ . Obviously, distinctions between resonant and off-resonant processes, above or below threshold etc. become meaningless.

An interesting implication for the theory of nonequilibrium processes is that, in such situations, also energy conservation has to be reconsidered. Results that involve the well-known “Fermi's golden rule” may lose their validity, as will be discussed in Chap. 6. All these effects will be an important issue in the short-time investigations, of the present book. To gain first insight, our analysis will concentrate on the simplest types of field-matter interaction, mainly on processes (iii)–(vi), in the nonrelativistic limit.

### 1.3.3 Overview of Relaxation Processes

**Excitation and relaxation.** Let us now return to the investigation of many-particle systems being brought out of equilibrium by some external excitation (e.g. a laser pulse) and consider the relaxation into a new stationary state. The character of this process depends strongly on the relevant time scales  $\tau_p$ ,  $t_{\text{rel}}$  and  $\tau_{\text{cor}}$ —the duration of the excitation (pulse duration) and the relaxation and correlation time<sup>23</sup> of the particle system. If  $\tau_p \ll \tau_{\text{cor}}$ , the excitation is “instantaneous”, and the relaxation starts from some initial state created by the excitation. In the opposite limit,  $\tau_p \gg t_{\text{rel}}$ , the excitation is quasistationary, and the system is effectively in equilibrium at all times, where the equilibrium state changes slowly with the excitation. Inbetween both limits, excitation and relaxation cannot be separated. This is the most interesting, but, at the same time, the most difficult situation.

**Time scales of relaxation processes.** While  $\tau_p$  is determined by the technical characteristics of the exciting laser, the relaxation time varies from one system to another and also with the parameters, such as density, chemical composition (e.g. degree of ionization) etc. Figure 1.8 shows typical values of the relaxation time for different systems (see bottom). For example, electron-hole plasmas in semiconduc-

---

<sup>23</sup>There may be various relaxation times, each related to another relaxation mechanism. Here, we have in mind the relaxation time of the momentum distribution. Typically  $\tau_{\text{cor}} < t_{\text{rel}}$ . We will discuss these time scales more in detail in Chap. 5.

tors have a lifetime<sup>24</sup> in the range of  $10^{-9} \dots 10^{-6}$  s. Typical relaxation times are in the range from 100 fs (at high densities of the order of  $10a_B^{-d}$ , where  $d$  is the dimensionality of the structure) to several picoseconds (at low densities,  $n < 0.1a_B^{-d}$ ). On the other hand, dense plasmas have a very broad range of relaxation times: for example, for fully ionized hydrogen  $t_{rel} \sim 10$  fs at a density of about  $10^{20} \text{ cm}^{-3}$ , and it decreases continuously with increasing density. The shortest relaxation times are found in nuclear matter, they are around  $10^{-23} \dots 10^{-22}$  s. Thus, interesting overlap of relaxation (and correlation) times with the pulse duration of modern lasers is observed in plasmas of moderate density and, especially, in condensed matter systems.

**Relaxation mechanisms.** In general, a laser pulse activates several relaxation mechanisms of the many-particle system at once. This depends mainly on the kinetic energy gained by the electrons and other particles during the excitation. For many processes, a threshold energy is required. This includes photo-ionization or impact ionization of bound states (atoms or molecules—in gases or plasmas; excitons, impurities and so on—in solids) or excitation of collective modes, such as vibrations of atoms in a molecule or in the crystal lattice (phonons) or of the charged particle gas (plasmons). Here, the typical energy exchanged between the electrons and the scattering partner is the phonon energy  $\hbar\omega_{ph}$  or the plasmon energy,  $\hbar\omega_{pl}$ , respectively.

The most important and general mechanism in a many-particle system is carrier-carrier scattering, e.g. electron-electron, electron-ion(or hole) and hole-hole (ion-ion) scattering. Here, the typical scattering energies are proportional to the scattering cross section  $\sigma$ , e.g. for Coulomb interaction in second Born approximation,<sup>25</sup>  $\sigma \sim V_{ab}^2(q) = [4\pi e_a e_b / \epsilon q]^2$ . From this expression it is clear that in systems with large background dielectric constant,  $\epsilon_b$ , (e.g. fluids or dielectrics) the energy exchange is strongly reduced and, therefore, the relaxation towards equilibrium takes longer. Another carrier-carrier scattering mechanism is the excitation of collective modes of the plasma (plasma oscillations, instabilities and so on), where the energy transfer is of the order of the plasmon energy  $\hbar\omega_{pl}$ . Typical values for the plasmon and phonon energies are indicated in Fig. 1.8. (lower left part). In this book, we will concentrate on carrier-carrier scattering and the underlying correlations. For a discussion of other scattering mechanisms in semiconductors and plasmas, see, respectively [63] and [31].

Finally we mention that, usually, there exists a *hierarchy* of relaxation processes with respect to the typical time, length or energy scales, which greatly simplifies the theoretical treatment of the relaxation, for details see Chap. 5.

<sup>24</sup>This is the time that proceeds, on average, until an electron recombines from the conduction band to the valence band. Note that drastically increased exciton life times exist in the case of “indirect excitons” predicted by Lozovik [59] where electrons and holes are spatially separated, either by an electric field [60] or by a buffer layer [61, 62].

<sup>25</sup>An improved treatment leads to cross sections in T-matrix approximation, see Chap. 9.

## 1.4 The Boltzmann Equation—Successes and Failure

The first in-depth analysis of the relaxation of a many-body system to equilibrium was performed by Ludwig Boltzmann [13] who derived an equation of motion for the single-particle probability density,  $f(\mathbf{r}, \mathbf{p}, t)$ . More precisely,  $df(\mathbf{r}, \mathbf{p}, t) = f(\mathbf{r}, \mathbf{p}, t)d^3rd^3p$  is the number of particles that occupies the phase space volume element  $d^3rd^3p$  at the point  $(\mathbf{r}, \mathbf{p})$  at time  $t$ . The total probability density is normalized to the particle number,  $\int d^3p d^3r f(\mathbf{r}, \mathbf{p}, t) = N$ .

### 1.4.1 An Elementary Introduction to the Boltzmann Equation

The equation of motion of the statistical quantity  $f(\mathbf{r}, \mathbf{p}, t)$  is readily formulated, starting from the  $N$ -particle distribution function  $f_N$ . This function is similar to  $f$  with the difference that it depends on the phase space coordinates of all  $N$  particles,  $f_N = f_N(\mathbf{r}_1, \mathbf{p}_1, \dots, \mathbf{r}_N, \mathbf{p}_N, t)$ . This function is well known from classical statistical mechanics, and it is equivalent to the exact solution of the  $N$ -particle problem for a given Hamiltonian of  $N$  identical particles

$$H_N = \sum_{i=1}^N \frac{\mathbf{p}_i^2}{2m} + \sum_{i=1}^N V(\mathbf{r}_i) + \frac{1}{2} \sum_i \sum_{j \neq i} W(\mathbf{r}_i, \mathbf{r}_j, ) \quad (1.4)$$

that are subject to an external potential  $V$  and interact via a pair potential  $W$ . The equation of motion of  $f_N$  follows from particle number conservation: its total differential vanishes<sup>26</sup>

$$0 = \frac{df_N}{dt} = \frac{\partial f_N}{\partial t} - \{H_N, f_N\}, \quad (1.5)$$

$$\{A, B\} = \sum_{i=1}^N \left[ \frac{\partial A}{\partial \mathbf{r}_i} \frac{\partial B}{\partial \mathbf{p}_i} - \frac{\partial B}{\partial \mathbf{r}_i} \frac{\partial A}{\partial \mathbf{p}_i} \right], \quad (1.6)$$

where in (1.6) we introduced the Poisson bracket. Using the Hamiltonian (1.4), we readily obtain the derivatives<sup>27</sup>

$$\frac{\partial H_N}{\partial \mathbf{p}_i} = \frac{\mathbf{p}_i}{m} = \mathbf{v}_i, \quad \frac{\partial H_N}{\partial \mathbf{r}_i} = -\frac{dV(\mathbf{r}_i)}{d\mathbf{r}_i} - \sum_{j \neq i} \frac{dW(\mathbf{r}_i, \mathbf{r}_j)}{d\mathbf{r}_i} = \mathbf{F}_i^{\text{ext}} + \mathbf{F}_i^{\text{int}}, \quad (1.7)$$

<sup>26</sup>This is the case if there are no particle creation or annihilation processes in the system.

<sup>27</sup>We assume  $W(\mathbf{r}_i, \mathbf{r}_j) = W(\mathbf{r}_j, \mathbf{r}_i)$ .

where we introduced the forces acting on particle “*i*” that are created by the external potential and all other particles, respectively.

Let us start by considering the case  $N = 1$ . Then, of course, interaction terms are missing, i.e.  $W \equiv 0$  and  $F^{\text{int}} \equiv 0$ . Introducing the results (1.7) in (1.5) we obtain

$$0 = \left\{ \frac{\partial}{\partial t} + \mathbf{v}_1 \frac{\partial}{\partial \mathbf{r}_1} - \frac{1}{m} \mathbf{F}_1^{\text{ext}} \frac{\partial}{\partial \mathbf{v}_1} \right\} f(\mathbf{r}_1, \mathbf{p}_1, t). \quad (1.8)$$

This can be interpreted as a continuity equation in phase space: the probability density at point  $(\mathbf{r}_1, \mathbf{p}_1)$  changes in time due to particle fluxes (the term with  $\partial_{\mathbf{r}_1} f$ ) and due to the external force (flux in momentum space, term with  $\partial_{\mathbf{v}_1} f$ ). This picture is complete for just a single particle.

However, if we consider a particle in the presence of other particles, the balance equation (1.8) will change. We can easily understand the qualitative structure of the equation in this case. The first effect is that the total force on particle “1” now is the sum of external force plus all interaction forces, cf. (1.7). This means, particle “1” (and any other) moves in a total field created by the force  $\mathbf{F}_1^{\text{ext}} + \mathbf{F}_1^{\text{int}}$ . The field due to  $\mathbf{F}_1^{\text{int}}$  is usually called “mean field”, as it describes the action of all particles in an average way.<sup>28</sup> Obviously, this mean field force of all particles cannot capture their total action on particle “*i*”, in particular, it neglects collision effects that take place upon close encounters. These collision effects will lead to an additional temporal change of the distribution function  $f$  which is denoted by  $\frac{\partial f}{\partial t}|_{\text{coll}}$  and is usually called “collision integral”. This effect “beyond mean-field” is called “correlation effect”, cf. Sect. 2.5. Thus the final form of the equation of motion of the one-particle distribution function—the kinetic equation—is

$$\left\{ \frac{\partial}{\partial t} + \mathbf{v}_1 \frac{\partial}{\partial \mathbf{r}_1} - \frac{1}{m} \mathbf{F}_1^{\text{ext}} \frac{\partial}{\partial \mathbf{v}_1} \right\} f(\mathbf{r}_1, \mathbf{p}_1, t) = \frac{\partial f}{\partial t}|_{\text{coll}} = I(\mathbf{r}_1, \mathbf{p}_1, t). \quad (1.9)$$

The collision integral takes into account all possible two-particle scattering events where the two particles that have, originally, the momenta  $\mathbf{p}_1^{\text{in}}, \mathbf{p}_2^{\text{in}}$  scatter into the momenta  $\mathbf{p}_1^{\text{final}}, \mathbf{p}_2^{\text{final}}$ . Since we want to know how the number of particles in momentum state  $\mathbf{p}_1$  changes, one of the momenta is fixed correspondingly. Thereby the momentum of the scattering partner (which will be denoted by  $\mathbf{p}_2$ ) is arbitrary, so we have to sum (integrate) over all possible values. Similarly we have to integrate over the momenta of the two particles  $(\bar{\mathbf{p}}_1, \bar{\mathbf{p}}_2)$  following the scattering event. Since this process reduces the number of particles in the state  $\mathbf{p}_1$ , this term enters with a sign minus. By symmetry, we also have to consider processes starting with momenta  $\bar{\mathbf{p}}_1, \bar{\mathbf{p}}_2$  and ending in the states  $\mathbf{p}_1, \mathbf{p}_2$  which will increase the population of state  $\mathbf{p}_1$  and, therefore, enter with the plus sign. The final step is to count the number of different microscopic scattering events which is easily done by multiplying with  $f(\mathbf{r}, \mathbf{p}, t)$  – the number of particles occupying the corresponding momentum state

<sup>28</sup>How exactly this averaging procedure is performed will be discussed in detail in Chap. 2, and the definition of the mean-field potential will be given in Sect. 2.5.

$$I(\mathbf{r}_1, \mathbf{p}_1, t) = \int d^3 p_2 \int d^3 \bar{\mathbf{p}}_1 \int d^3 \bar{\mathbf{p}}_2 P(\mathbf{p}_1, \mathbf{p}_2; \bar{\mathbf{p}}_1, \bar{\mathbf{p}}_2) \\ \times \{f(\mathbf{r}_1, \bar{\mathbf{p}}_1, t) f(\mathbf{r}_1, \bar{\mathbf{p}}_2, t) - f(\mathbf{r}_1, \mathbf{p}_1, t) f(\mathbf{r}_1, \mathbf{p}_2, t)\}. \quad (1.10)$$

Here we introduced an additional function  $P$  that properly accounts for the fact that different scattering processes may have different probabilities.<sup>29</sup>

Equation (1.9) with the collision integral (1.10) is a very general result for classical many-particle systems and has been used very successfully during the recent century. At the same time, these equations miss key features of quantum many-body systems in general and correlated systems, in particular. The main problems are

1. For quantum systems the mean field term on the l.h.s. of (1.8) has a more complicated form (it is non-local) due to the finite extension of quantum particles.
2. Indistinguishability of quantum particles gives rise to an additional mean field-type term—the exchange (Fock) contribution.
3. Quantum exchange also affects the form of the collision integral (1.10). There appear additional factors of the form  $1 \pm f$  that take into account that, for fermions (minus sign), occupied states cannot be occupied by a second particle the Pauli principle.
4. An even more fundamental problem is that the collision integral (1.10) does not satisfy the correct conservation laws of a nonideal system.

Finally, these equations are not applicable to ultra-short time scales and ultrafast processes, as will be shown in Sect. 1.4.2. So there is more than enough reason to look for generalizations of these equations which is the subject of the present book. The problems related to the non-locality (1. above) will be solved in Sect. 2.3.2 whereas exchange effects (points 2. and 3.) are the subject of Chap. 3. The issue of the conservation laws for quantum kinetic equations will be analyzed in Chap. 8.

While we have written down a rather general form of the collision integral, (1.10), the explicit form of the probability  $P$  may strongly vary, depending on the physical system. It crucially depends on the type and range of interaction and on the coupling strength. Various important cases will be studied in detail in the various chapters of this book. Here we consider, as an example, the case of charged particles that interact via the Coulomb potential. In this case, straightforward application of perturbation theory yields<sup>30</sup>

$$P \sim \tilde{W}^2 \delta(\bar{\mathbf{p}}_1 + \bar{\mathbf{p}}_2 - \mathbf{p}_1 - \mathbf{p}_2) \delta(\bar{E}_1 + \bar{E}_2 - E_1 - E_2), \quad (1.11)$$

where  $\tilde{W}(q) = \frac{4\pi e^2}{q^2}$  is the Fourier transform of the Coulomb potential. Here  $\mathbf{q} = \bar{\mathbf{p}} - \mathbf{p}$  is the momentum transferred between the particles during the scattering event, and the delta functions indicates that the total momentum of the two particles and their total energy,  $E_1 + E_2$ , are conserved. However, using this result for  $P$  it was quickly

<sup>29</sup>For simplicity we assumed that  $P$  is symmetric with respect to the exchange  $\mathbf{p}_1, \mathbf{p}_2 \leftrightarrow \bar{\mathbf{p}}_1, \bar{\mathbf{p}}_2$  and does not explicitly depend on the position and time instance of the scattering process.

<sup>30</sup>This will be derived in Chap. 6.

observed that the collision integral (1.10) diverges. The reason is the long range of the Coulomb interaction which falls off like one over the distance. This divergence is not a true physical effect but a deficiency of the approximation: in a plasma, the long-range Coulomb force gives rise to accumulation of oppositely charged particles around a given charge—i.e. to screening. As a consequence, the net potential becomes modified according to<sup>31</sup>  $\tilde{W}(q, \omega) \rightarrow \tilde{W}^s(q) = \tilde{W}(q)/\epsilon(\omega, q)$ . The screening effect of the surrounding plasma is captured by the dielectric function  $\epsilon$ . It reduces the range of the original potential and, at the same time, takes into account collective properties of the plasma (plasma oscillations) which are related to the frequency dependence.<sup>32</sup>

### 1.4.2 Unphysical Ultrafast Relaxation in Charged Particle Systems

A kinetic equation with the dynamically screened potential  $W^s$  was first derived in 1960 by Balescu [64] and Lenard [65] and analyzed by many plasma physicists in detail. However, a full numerical solution of the corresponding kinetic equation with a collision integral involving  $W^s$  turned out to be very difficult due to the existence poles of  $W^s$ . The first solutions for a two-component quantum system (electron-hole plasma) in optically excited semiconductors were reported by Binder et al. 30 years later [66, 67]. They made an unexpected observation: the distribution function of electrons and holes which is created by a laser pulse relaxed, in some cases, extremely fast to equilibrium. The character (relaxation) time was found to be as short as few tens of femtoseconds and even several femtoseconds, an example is shown in Fig. 1.9. This was in striking contrast experiments with optically excited semiconductors showing relaxation times in the range of 100–500 fs.

This discrepancy between experiment and theory has triggered a large amount of theoretical work during the next decade. This obvious failure of the Boltzmann equation<sup>33</sup> was unexpected since it was thought to be the most advanced quantum kinetic approach available. The solution of this dilemma is the following: during the laser excitation, electrons (holes) are gradually created in the conduction (valence) band. During this finite time also the rearrangement of particles takes place that gives rise to the formation of the screening “cloud” around each individual particle. This means the dielectric function is also gradually being built up during this time.<sup>34</sup> However, this process of the formation of screening (and more generally, formation of correlations) is neglected in the Boltzmann equation with the collision integral (1.10) because all scattering events are treated as instantaneous.

<sup>31</sup>The dynamically screened collision integral will be studied in Chap. 10.

<sup>32</sup>This will be studied in detail in Chap. 4.

<sup>33</sup>The kinetic equation with the Lenard-Balescu collision term involving  $W^s$  is often called Boltzmann equation, in the semiconductor community.

<sup>34</sup>The first numerical treatment of this process was accomplished by Banyai et al. [68] and verified experimentally by Leistenstorfer et al. [69]. We will discuss this issue in detail in Chaps. 10 and 13.

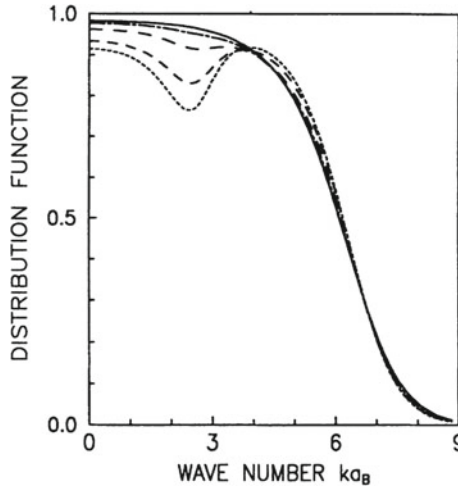


**Fig. 1.9** Relaxation of the electron distribution function in an optically excited semiconductor. The initial distribution has a double peak structure where the high-momentum peak is determined by the photon energy in excess to the band gap. Due to electron-electron scattering the distribution relaxes towards a Fermi function. Consecutive times are  $t = 21$  fs (*short-dashed line*),  $t = 75$  fs (*long-dashed line*), and  $t = 147$  fs (*dash-dotted line*), and the final time  $t = 796$  fs. Solutions of the quantum Lenard-Balescu equation. Figure reprinted with permission from [67]. Copyright (1992) by the American Physical Society

From this example we conclude that the kinetic equations (classical or quantum) with such Boltzmann-type collision integrals are not applicable to ultrafast processes or to the early stage of time evolution. It is one of the main subjects of this book to derive generalized quantum kinetic equations that overcome these limitations. As we will see, there exists a straightforward way to accomplish this goal. At the same time, there exists a strict theoretical procedure with a clear set of approximations that are required in order to recover the conventional Boltzmann equation.

## 1.5 Improved Theoretical Concepts

The theoretical analysis of nonequilibrium behavior of many-particle systems is essentially more involved than the description of its equilibrium properties. Therefore, many of the methods discussed in Sect. 1.2 are not applicable to time dependent phenomena. Depending on the dominating relaxation mechanism, the theoretical treatment of the evolution towards equilibrium varies greatly. For situations which are close to equilibrium, one may use rate equations or hydrodynamic equations. If the momentum distributions of the particles deviate significantly from the equilibrium distribution, the appropriate concept are kinetic equations, such as the Boltzmann



equation discussed above in Sect. 1.4. However, as was mentioned in the beginning, conventional kinetic equations have two major deficiencies:

- A. They assume implicitly that all correlations have already reached their equilibrium form (in particular, they assume that initial correlations are completely weakened), and thus they are not applicable to times shorter than the correlation time, and
- B. They conserve only kinetic (single-particle) energy and are, therefore, not applicable to correlated many-particle systems. In particular, they yield the equilibrium distribution of an ideal gas, completely neglecting correlation corrections.

In fact, we will see that both points are very closely related. Therefore, the description of ultrafast processes ( $t < \tau_{cor}$ ) as well as the relaxation of strongly coupled systems, both, require generalized kinetic equations. Derivation, investigation and numerical solution of these equations is the main topic of this book. But before we give an outline, it is appropriate to summarize some of the important early results in this field.

**Historical remarks.** A straightforward extension of equilibrium theories to non-equilibrium is the *Linear response* approach developed by Kubo, Mori, Zubarev and others, e.g. [70, 71]. This approach uses a generalized equilibrium statistical operator which depends on additional observables. This method has been very successful for the description of transport processes in correlated systems close to equilibrium, see also [31, 72, 73, 74, 75].

A very general nonequilibrium method is based on the hierarchy of equations for the reduced *density operators*, the *BBGKY-hierarchy*, which was developed by Bogolyubov, Born, Green, Kirkwood, Yvon and others, e.g. [76, 77] and which was later generalized to quantum systems. It is well suited for the derivation of generalized quantum kinetic equations. Furthermore, there have been proposed other concepts to derive *Generalized (non-Markovian) kinetic equations*, by Prigogine [78], Resibois [79], Zwanzig [80], Balescu [81], Klimontovich and Silin [82] and others.<sup>35</sup> Klimontovich developed the *method of microscopic phase space densities* [83] which proved to be very general<sup>36</sup> and allowed him to derive a great variety of generalized kinetic equations for nonideal gases and plasmas [72]. Bärwinkel and Grossmann were the first to show that total energy conservation in kinetic equations is closely related to the time structure (non-Markovian or retardation effects) of the collision integral [84, 85].

---

<sup>35</sup>In particular, the kinetic equations derived by Prigogine contain an initial correlation term and a non-Markovian scattering term  $dF(t)/dt = I_{IC}(t - t_0) + \int_{t_0}^t d\tau K(t - \tau)F(\tau)$ . It could be shown in very general form that the initial correlation term is damped. We will recover this general form from the BBGKY-hierarchy in Chap. 7.

<sup>36</sup>The fluctuating phase space density is defined in the  $6N$ -dimensional phase space  $[x = (\mathbf{r}, \mathbf{p})]$  according to  $N(x, t) = \sum_{i=1}^N \delta[x - x_i(t)]$ , where  $x_i(t)$  is the exact trajectory of particle “i”. This method straightforwardly incorporates density and field fluctuations and is, in fact, the classical analogue to the second quantization method of field theory.

A powerful approach to generalized quantum kinetic equations which derived from field theory is the method of *Nonequilibrium Green functions*. Here, major contributions are due to Martin and Schwinger [86, 87], Kadanoff and Baym [45, 88], Keldysh [89]. The incorporation of electromagnetic fields was studied by Korenman [90] and Dubois [91]. Extensions to the relativistic case have been developed by Akhiezer and Berestezki [92] as well as Dubois and Bezzerides [91, 93], following the early papers of Schwinger [94, 95].

Finally, nonequilibrium processes are successfully treated within purely mechanical concepts, i.e. by *Molecular Dynamics simulations*. These methods are very straightforward in application to classical particles where they yield very high accuracy results. The extension of these techniques to quantum systems is currently actively discussed.<sup>37</sup>

Summarizing these developments, we conclude that today there exist three major approaches that are applicable to ultrafast phenomena:

- I. Density operator techniques. BBGKY-hierarchy;
- II. Nonequilibrium Green functions theory;
- III. Classical and Quantum Dynamics simulations.

Naturally, we can mention only a very small part of the tremendous literature. Further references will be given in the chapters below (for additional literature on correlation effects in strongly coupled plasmas, solids and nuclear matter, see, respectively, [23, 31, 63, 96]. For completeness, we mention that there exist excellent investigations of ultrafast phenomena which use Monte Carlo techniques, which we cannot discuss here, see e.g. [97] and references therein. This approach is closely related to points I. or II., since it is based on quantum kinetic equations too. Other rapidly developing approaches are time-dependent density functional theory [98] or time-dependent extensions of the density renormalization group approach [99], for an overview, see [100].

### 1.5.1 Outline of this Book

We will consider all three methods highlighted above, although we focus on the density operator approach, because it is conceptually simple. In Chaps. 2 and 3, we give a detailed introduction into the method of reduced density operators, based on the BBGKY-hierarchy, discuss its properties, the treatment of correlations and important decoupling approximations. In Chap. 3 we generalize these results by the incorporation of spin statistics effects.

In Chaps. 4–11, we discuss important approximations, beginning with the mean-field (Hartree/Vlasov) approximation, which describes collective phenomena (plasmons) in the absence of correlations. Correlation effects are introduced in

---

<sup>37</sup>In the first edition of this book we have compared the underlying concepts of the dynamical and the statistical approaches in detail. In the mean time there has been ongoing activity in this rapidly growing field which cannot be adequately covered here.

Chaps. 5 and 6 and discussed further in Chap. 7, where we focus on Non-Markovian behavior and selfenergy. In Chap. 8 we discuss important properties of quantum kinetic equations before the discussion is extended to more complex correlation phenomena in Chaps. 9–11. This will include strong correlations and bound states as well as dynamical screening and screening buildup.

The consistent incorporation of electromagnetic fields into the BBGKY-hierarchy and the derivation of generalized Bloch equations is the subject of Chap. 13 and concludes our discussion of the density operator approach.

The method of nonequilibrium Green functions is summarized in Chap. 13, where we start from a fully relativistic formulation. We derive the relativistic Keldysh-Kadanoff-Baym equations for particles and photons and their nonrelativistic limit and compare the Green functions results to those of the density operator theory.

## 1.6 Problems

**Problem 1.1** Find the connection between the two quantum degeneracy parameters,  $\chi$  and  $\Theta$ , cf. (1.2).

**Problem 1.2** Find the relation between the two quantum coupling parameters,  $\Gamma_q$  and  $r_s$ , cf. (1.3).

**Problem 1.3** Compute the average energy gain of a classical charged particle in the field of a monochromatic linearly polarized laser field .

<http://www.springer.com/978-3-319-24119-7>

Quantum Kinetic Theory

Bonitz, M.

2016, XVIII, 406 p. 61 illus., 52 illus. in color., Hardcover

ISBN: 978-3-319-24119-7